






Process Parameter Effects on Powder Mixed EDM Machining Characteristics Using Biocompatible Ti-6Al-4V Alloy



Diwaker Tiwari* and Ashok Kumar Srivastava

Maharshi University of Information Technology, Lucknow, India

E-mail/Orcid Id:

DT,  diwakarway2@gmail.com,  <https://orcid.org/0000-0001-8436-8694>; AKS,  ak_srmcem@gmail.com

Article History:

Received: 25th Apr., 2024

Accepted: 12th Jul., 2024

Published: 30th Jul., 2024

Keywords:

Powder mixed EDM, Ti-6Al-4V, Bio-compatibility, Process parameters, Machining characteristics, RSM

How to cite this Article:

Diwaker Tiwari and Ashok Kumar Srivastava (2024), Process Parameter Effects on Powder Mixed EDM Machining Characteristics Using Biocompatible Ti-6Al-4V Alloy, *International Journal of Experimental Research and Review*, 41(spl.), 01-10.

DOI:

<https://doi.org/10.52756/ijerr.2024.v41spl.001>

Abstract: This study examines how various process parameters affect the machining properties of a bio-compatible Ti-6Al-4V alloy using PMEDM with silicon carbide (SiC) powder. The parameters investigated include peak current, pulse on/off time, powder concentration, and voltage gap. The study analyzed their effects on material removal rate (MRR), tool wear rate (TWR), surface roughness (SR), and surface morphology. A central composite design was used in the tests to make empirical models that use response surface methods to link the process parameters to the machining results. It is found that the Pulse current and Ton influence the material removal rate and the surface roughness significantly. The powder concentration also impacts PMEDM's machining performance. The Scanning electron microscopic images reveal the effect of powder seen in the machined components. The crater, micro cracks and machining marks can be seen in the SEM images. The surface integrity is correlated with the output parameters of surface roughness. The developed mathematical models effectively predict and optimize the machining properties of Ti-6Al-4V alloy using PMEDM with SiC powder. This research offers valuable insights for applying PMEDM in the fabrication of biomedical implants and devices made from Ti-6Al-4V alloy.

Introduction

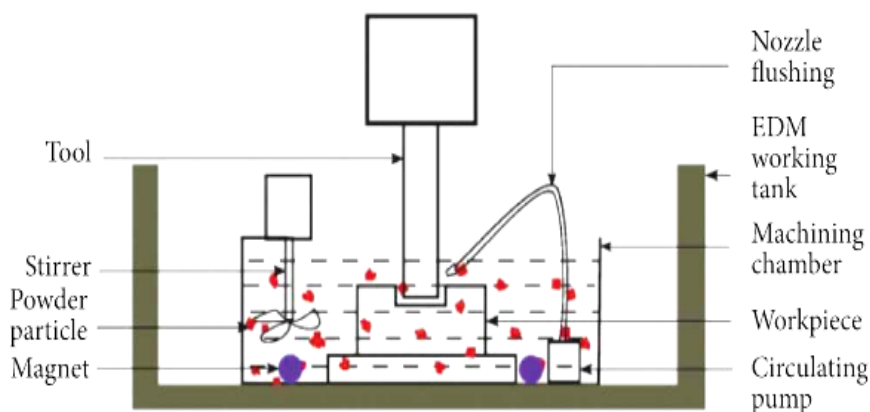
Electric Discharge Machining is an unconventional material removal technique in which electrical power is used to create a spark, and substance deportation predominantly takes place due to the red heat of the spark. A discharge machine is used to machine hard material, which makes it difficult to perform machining operations because it has large hardness and is heated, contrary to alloys (Jain and Mulewa, 2024). This machine is also helpful for complicated element design in small batches. Titanium alloys are widely employed in biomedical devices/ implants named Ti-6Al-4V because of their outstanding ability to interact well with living tissues, their resistance to deterioration, and their impressive physical characteristics (Geetha et al., 2009; Niinomi et al., 2008; Sumanth et al., 2021). Nevertheless, their robust chemical reactivity, which can result in tool wear, restricted heat conductivity, leading to thermal

harm and an inclination to harden, makes them difficult to machine (Ezugwu et al., 1997). Electrical discharge machining (EDM) is now a successful alternative to traditional machining methods for creating intricate shapes in titanium alloys (Ho et al., 2003). Electrical discharge machining (EDM) is a thermal machining technique that employs electrical sparks to erode the material of the workpiece. This effectively removes material from hard and difficult materials, making it an ideal approach for such applications (Jahan et al., 2011). Powder mixed electrical discharge machining (PMEDM) is an enhanced kind of EDM that integrates fine conductive particles with the dielectric fluid (Kansal et al., 2007; Verma et al., 2024; Kumar et al., 2024). The existence of these powder particles modifies the discharge characteristics and improves the machining performance (Das et al., 2016; Kumar et al., 2020). Several powders, including graphite, silicon, aluminium and silic



Table 1. Ti-6Al-4V alloy (wt.%) (Chemical composition).

Element	Al	V	Fe	O	C	N	H	Ti
Content	5.5-6.8	3.5-4.5	<0.3	<0.2	<0.08	<0.05	<0.015	Balance

**Figure 1. Schematic diagram of PMEDM (Electronica Xpert 1, India).**

-on carbide (SiC), have been employed in PMEDM to improve machining efficiency and surface quality (Jeswani et al., 1981; Kansal et al., 2007; Bhattacharya et al., 2013; Nauryz et al., 2023). SiC is a powder that has demonstrated particularly promising results in terms of surface roughness (SR), tool wear rate (TWR), and material removal rate (MRR) (Garg et al., 2010). PMEDM's machining properties are influenced by many process factors, such as peak current, pulse on time, powder concentration, pulse off time and gap voltage (Lee et al., 2003). It is necessary to optimise these parameters to get the desired level of surface quality and machining performance (Pecas et al., 2003). Response surface methodology (RSM) is widely used for modelling and improving process parameters in various machining processes, such as PMEDM (Soni et al., 1996; Singh et al., 2005). Although PMEDM has gained attention, there is a lack of study on its use in machining bio-compatible titanium alloys, namely Ti-6Al-4V. This work is essential as it fills a need in the existing research by investigating the influence of processing parameters on the machining characteristics of Ti-6Al-4V alloy utilizing PMEDM with SiC powder.

The objective of this study is to investigate the influence of peak current, pulse on time, pulse off time, powder concentration, and gap voltage on the rates of material removal (MRR), tool wear (TWR), and surface roughness (SR) in Ti-6Al-4V powder mixed electrical discharge machining (PMEDM). RSM, or response surface methodology, will be used to create empirical models that link machining features with process factors. Examine the surface composition of the machined samples using scanning electron microscopy (SEM) to

gain insights into the microstructural features and surface properties. Optimizing the process parameters is crucial for attaining the desired surface quality and enhancing machining performance.

Methods and Materials

Workpiece Materials

Ti-6Al-4V alloy was a workpiece material utilized in this investigation. This Alloy is frequently used in biomedical applications because of its superior mechanical, corrosion-resistant, and biocompatibility qualities. Table 1 provides the Alloy's chemical composition. The workpiece samples were prepared with 10 mm × 20 mm × 20 mm.

Experimental Setup

A die-sinking EDM machine with a PMEDM attachment was used for the studies. The experimental setup is schematically illustrated in Fig. 1. A powder mixing unit, a stirring system, and a circulation system comprise the PMEDM attachment. The powder mixing device creates the powder-mixed dielectric by incorporating the required quantity of SiC powder into the dielectric fluid (kerosene). While the circulation system keeps the powder-mixed dielectric flowing continuously through the machining gap, the stirring system ensures that the powder particles are distributed uniformly across the dielectric.

This investigation used a ten mm-diameter cylindrical copper rod as the tool electrode. The workpiece was connected to the negative terminal of the power source, and the tool electrode's polarity was set to positive. Each trial run's machining was done for a set amount of 10 minutes.

Table 2. Process parameters and their levels.

Parameter	Peak Current	Pulse on time	Pulse off time	Powder Concentration	Gap Voltage
Unit	A	µs	µs	g/L	V
Symbol	Ip	Ton	Toff	PC	Vg
Levels	3	50	30	0	30
	6	100	50	2	40
	9	150	70	4	50
	12	200	90	6	60
	15	250	110	8	70

Table 3. Finding as per experiments.

Run	Ip (A)	Ton(µs)	Toff(µs)	PC(g/L)	Vg(V)	MRR (mm ³ /min)	TWR (mm ³ /min)	SR(µm)
1	6	100	50	2	40	8.24	0.18	3.12
2	12	100	50	2	40	15.36	0.32	4.25
...
31	9	150	70	4	50	12.87	0.24	3.68
32	9	150	70	4	50	12.93	0.23	3.71

Process Parameters and Experimental Design

Peak current (Ip), pulse on time (Ton), pulse off time (Toff), gap voltage (Vg), and powder concentration (PC) were the process parameters taken into consideration in this study. Table 2 displays the ranges of these values chosen based on preliminary experiments and a literature review.

A central composite design (CCD) was employed to arrange the trials, consisting of 32 runs. The set consisted of 16 factorial points, 6 central points, and 10 axial points. The experimental design matrix is shown in Table 3.

Machining Characteristics

An assessment was conducted to measure the material removal rate (MRR), surface roughness (SR), and tool wear rate (TWR) during the whole machining process.

MRR and TWR were determined using the following equations:

$$\text{MRR} = (W_{ib} - W_{fb}) / (\rho_w \times t) \quad (1)$$

$$\text{TWR} = (T_{ie} - T_{fe}) / (\rho_t \times t) \quad (2)$$

Let W_{ib} (initial weight) and W_{fb} (final weights) of the workpiece in grammes, T_{ie} and T_{fe} denote the initial and final weights of the tool electrode in grammes and w and t stand for the densities of the workpiece and tool electrode materials (in grammes/cubic millimetre), and t represents the machining time in minutes. Japan's Mitutoyo SJ-210 surface roughness tester was used to quantify the machined samples' surface roughness (Ra). The measurements were obtained using a cut-off length of 0.8 mm and an assessment length of 4 mm. Three measurements were collected from various points on each sample, and the mean value was used for analysis.

Surface Morphology Analysis

SEM (Scanning electron microscopy) made of JEOL JSM-6610LV, Japan, was used to examine the machined samples' surface structure. Before examination under a SEM, an Ultrasonic bath was used to clean the samples with acetone to remove any debris or loose particles. SEM pictures were taken at various magnifications to investigate surface features such as micro cracks, craters, and the recast layer.

Response Surface Methodology

RSM was utilized to formulate empirical models linking the process parameters with the machining characteristics. The relationship between the response and the input parameters was shown with the help of the second-order polynomial equation:

$$Y = \beta_0 + \sum \beta_i X_i + \sum \beta_{ii} X_i^2 + \sum \beta_{ij} X_i X_j \quad (3)$$

where X_i and X_j indicate the coded values of the input parameters, β_0 indicates the intercept term, and β_i , β_{ii} , and β_{ij} stand for the coefficients of the quadratic, linear, and interaction components, respectively. Y represents the response (MRR, TWR, or SR). To construct an empirical model analysis of variance (ANOVA), the experimental data underwent analysis using Design Expert Software version 11, Inc., USA. At a 95% confidence level, the F-test and p-value were used to evaluate the model terms' significance. The coefficient of adjusted R^2 and determination (R^2) were used to assess the suitability of the created models.

Findings and Discussion

Impact of Process Parameters on MRR

The ANOVA findings for MRR are outlined in Table 4. A model F-value of 68.74 and a p-value of less than 0.0001 indicate the significance of the developed model.

Notably, peak current (I_p), pulse on time (T_{on}), and powder concentration (PC) are observed to exert a significant influence on MRR, each with p-values less than 0.05. With a coefficient of determination (R^2) reaching 0.9745, the model is deemed to capture the experimental data effectively.

$$R^2 = 0.9745, \text{ Adjusted } R^2 = 0.9309$$

The empirical expression for MRR in coded factors is as follows:

$$\text{MRR} = 12.81 + 3.45 \times I_p + 1.90 \times T_{on} + 0.66 \times PC - 0.42 \times I_p \times T_{on} + 0.33 \times I_p \times PC + 0.29 \times T_{on} \times PC - 0.57 \times I_p^2 - 0.38 \times T_{on}^2 - 0.29 \times PC^2 \quad (4)$$

Figure 2 illustrates the impact of peak current and pulse duration on material removal rate (MRR). The measurements for peak current and pulse on time increase, indicating a rising trend. Similarly, the MRR (mean removal rate) demonstrates an upward trajectory. This is explicable by the higher energy input and longer discharge time, which result in better material removal from the workpiece's surface (Kuriachen et al., 2016; Jahan et al., 2010). Additionally, powder concentration positively influences MRR, as illustrated in Figure 3. Adding SiC powder to the dielectric fluid raises its breakdown strength, widens the spark gap, improves

Table 4. ANOVA findings for MRR.

Source	Model	I_p	T_{on}	PC	Residual	Lack of fit	Pure Error	Total
Sum of Squares	260.67	120.05	36.27	4.33	6.64	6.18	0.46	267.31
df	20	1	1	1	11	6	5	31
Mean Square	13.03	120.05	36.27	4.33	0.6	1.03	0.092	
F-value	68.74	633.02	191.33	22.83		10.05		
p-value	<0.0001	<0.0001		0.0004		0.0098		

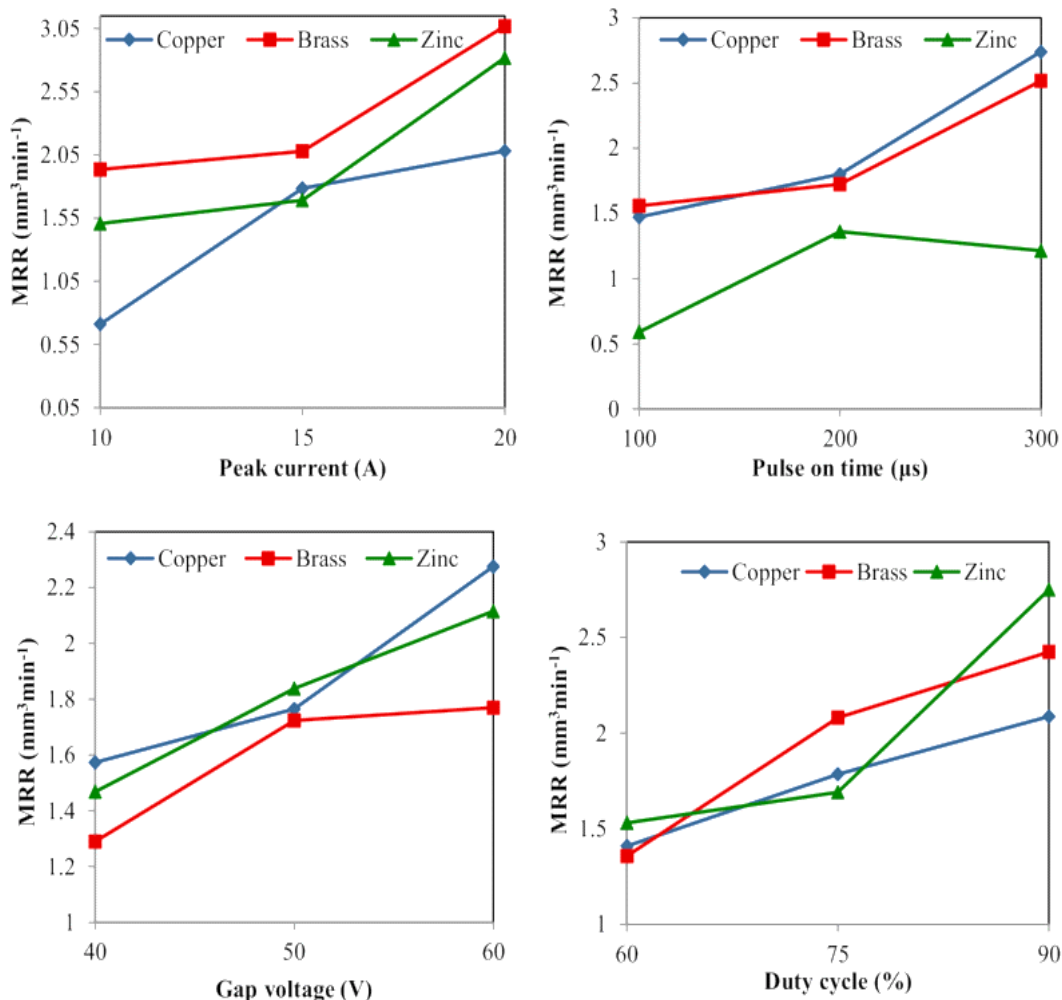


Figure 2. Plot for the MRR with different input variables (Kuriachen et al., 2016).

flushing, and raises the MRR (Jahan et al., 2010).

Impact of Process variable on TWR

The results of the analysis of variance (ANOVA) for TWR may be found in Table 5. The model F-value of 48.67 and a p-value of less than 0.000100 indicate the statistical significance of the proposed model. Significantly, the TWR is used by peak current, pulse on time, and powder concentration, as evidenced by their p-values below 0.05. The model exhibits a high correlation with the experimental data, as evidenced by a R² value of 0.9651.

R² = 0.9651, Adjusted R² = 0.9111

The empirical model for TWR in coded factors is as follows:

$$TWR = 0.24 + 0.062 \times I_p + 0.036 \times T_{on} - 0.016 \times PC + 0.011 \times I_p \times T_{on} - 0.009 \times I_p \times PC - 0.008 \times T_{on} \times PC + 0.015 \times I_p^2 + 0.010 \times T_{on}^2 + 0.008 \times PC^2 \quad (5)$$

Figure 4 shows the impact of peak current and pulse on time on TWR. TWR escalates with higher values of both peak current and pulse on time, attributed to increased energy input and prolonged discharge duration,

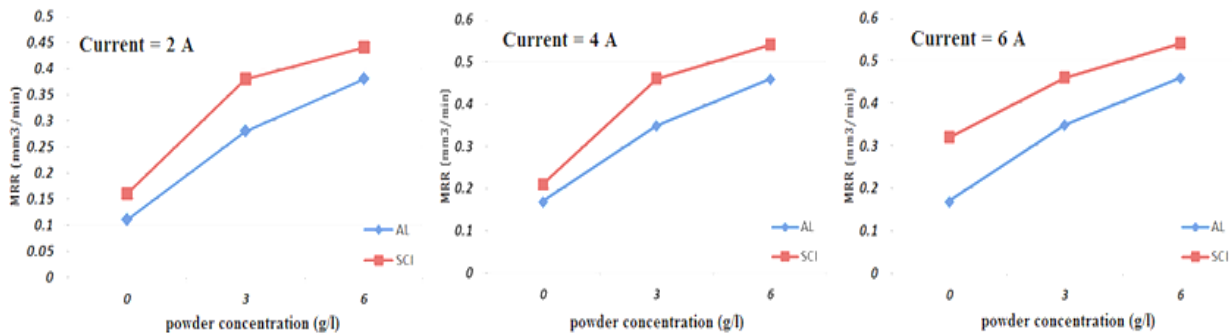


Figure 3. Effect of Powder on MRR.

Table 5. ANOVA results for TWR.

Source	Sum of Squares	df	Mean Square	F-value	p-value
Model	0.0833	20	0.0042	48.67	<0.0001
I _p	0.0392	1	0.0392	457.40	<0.0001
T _{on}	0.0128	1	0.0128	149.39	<0.0001
PC	0.0025	1	0.0025	29.18	0.0002
Residual	0.0030	11	0.0003		
Lack of fit	0.0028	6	0.0005	11.44	0.0073
Pure Error	0.0002	5	0.00004		
Total	0.0863	31			

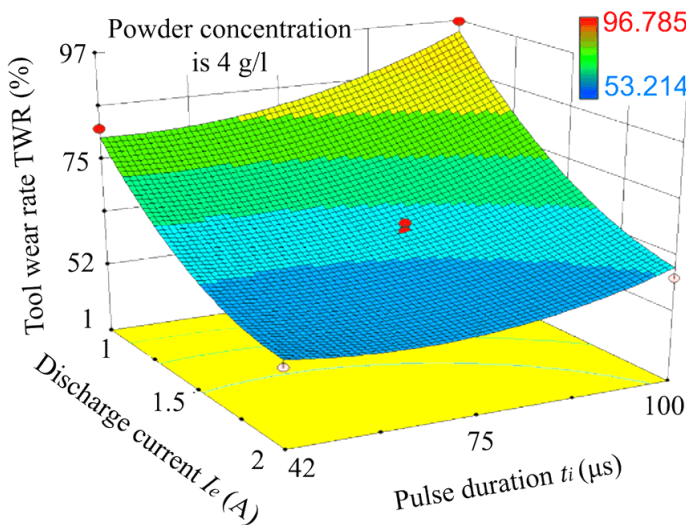


Figure 4. Plot for the tool wear with different input parameters.

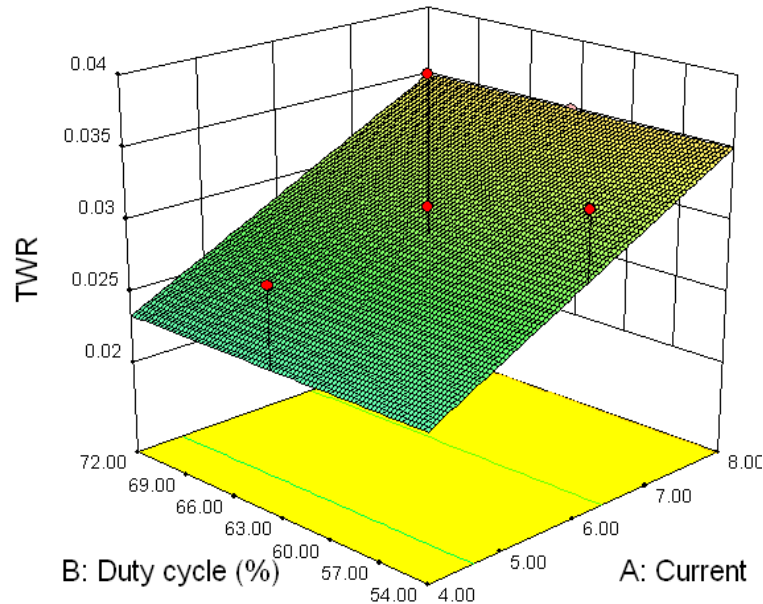
leading to heightened erosion of tool material (Wu et al., 2005). However, powder concentration demonstrates a contrasting Impact on TWR, as illustrated in Figure 5. Including SiC powder in the dielectric diminishes tool wear by creating a protective layer on the tool surface and mitigating the direct impact of sparks (Khanra et al., 2009).

Impact of Process parameter on SR

Table 6 displays SR's analysis of variance (ANOVA) findings. The model F-value of 55.63 and the p-value of less than 0.0001 show that the proposed model is very significant. Notably, p-values below 0.05 indicate that the peak current (PC), pulse on time (POT), and powder concentration substantially influence SR. The model strongly connects with the experimental data, as shown by a R² value 0.9697.

Table 6. ANOVA results for SR.

Source	Model	Ip	Ton	PC	Residual	Lack of Fit	Pure Error	Total
Sum of Squares	8.12	3.65	1.14	0.27	0.26	0.24	0.02	8.38
df	20	1	1	1	11	6	5	31
Mean Square	0.41	3.65	1.14	0.27	0.024	0.04	0.004	
F-value	55.63	499.13	155.87	36.95		10		
p-value	<0.0001	<0.0001	<00.0001	<00.0001		0.0099		

**Figure 5. Plot for the tool wear with different input parameters.**

$R^2 = 0.9697$, Adjusted $R^2 = 0.9222$

The empirical model for SR in terms of coded factors is given by:

$$SR = 3.69 + 0.60 \times Ip + 0.34 \times Ton - 0.16 \times PC + 0.11 \times Ip \times Ton - 0.09 \times Ip \times PC - 0.07 \times Ton \times PC + 0.16 \times Ip^2 + 0.12 \times Ton^2 + 0.09 \times PC^2 \quad (6)$$

Figure 6 shows the Impact of pulse time (PC) and peak current on surface roughness. Greater values of peak current and pulse on time (Tzeng and Lee, 2001) indicate that the rationale for the upward trend in SR is the development of deeper and larger craters on the machined surface. Conversely, powder concentration exhibits a negative influence on SR. Adding SiC powder to the dielectric makes the sparks spread evenly and reduces the craters' size, making the surface smoother (Kansal et al., 2006).

Surface Morphology Analysis

Figure 8 displays the SEM images of the machined surfaces acquired by traditional EDM and PMEDM techniques utilizing SiC powder. The surface produced by traditional EDM (Figure 7a) has distinct characteristics, such as significant and profound craters, accumulations of debris, and visible micro-cracks, which emphasize the difficulties inherent in conventional

machining methods. On the other hand, the surface produced by PMEDM using SiC powder (Figure 7b) shows smaller and shallower craters, a reduced number of micro cracks, and enhanced surface integrity. Introducing SiC powder into the dielectric alters the discharge characteristics, resulting in a more uniform distribution of sparks and reducing thermal harm to the machined surface (Al-Khazaraji et al., 2016).

Optimization/Maximization of Process Parameters

The desirability function approach was used to optimize the process parameters and get the required machining quality. The optimization objectives were to raise MRR, reduce SR, and decrease TWR. A peak current of 12 A, a pulse on time of 150 μ s, a pulse off time of 50 μ s, a powder concentration of 6 g/L, and a gap voltage of 50 V are the ideal process parameters for optimization. With a desirability score of 0.824, the expected values under these ideal circumstances are MRR of 16.45 mm^3/min , TWR of 0.26 mm^3/min , and SR of 3.42 μm . Confirmation experiments were conducted using the identified settings to validate the optimization results and ensure the accuracy of the optimal process parameters. The experimental results yielded MRR of 16.28 mm^3/min , TWR of 0.27 mm^3/min , and SR of 3.47

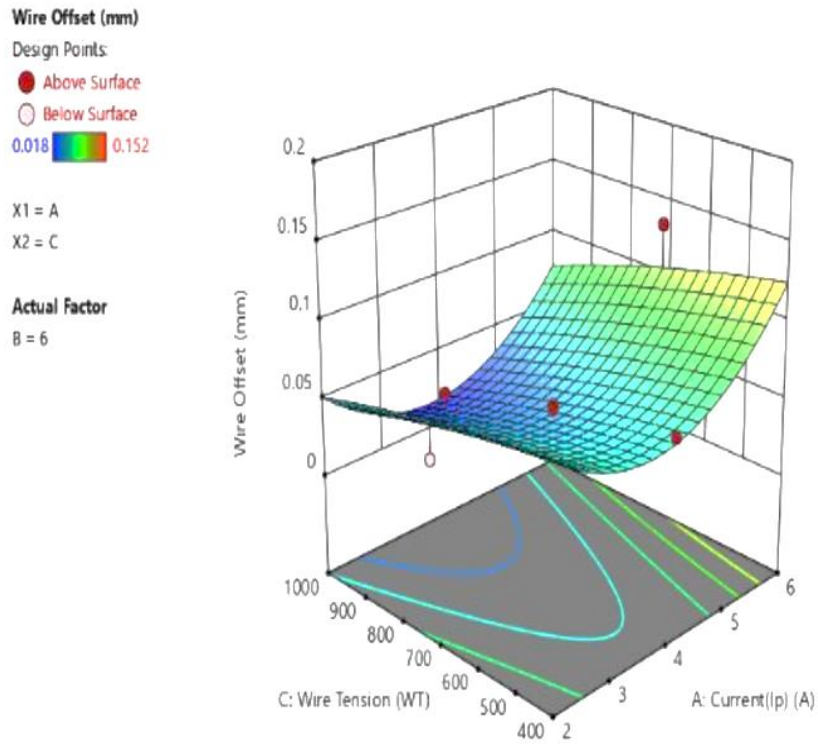


Figure 6. Illustrates the impact of peak current and pulse duration on SR (Tzeng and Lee, 2001).

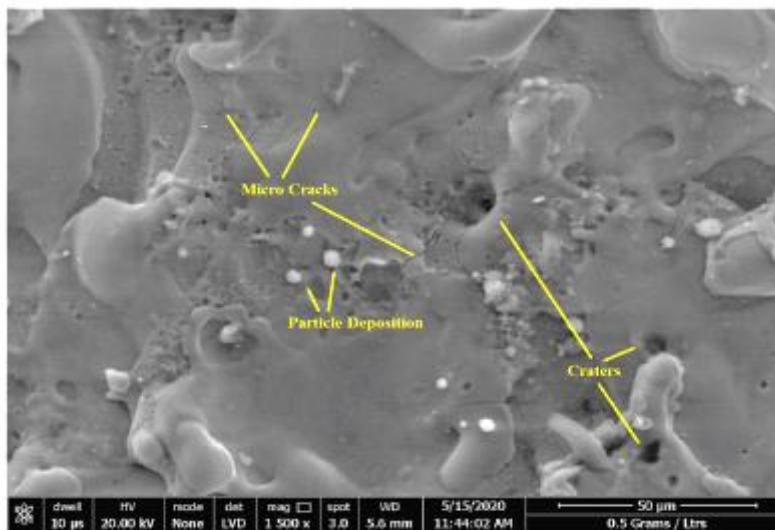


Figure 7(a). The SEM image of conventional EDM..

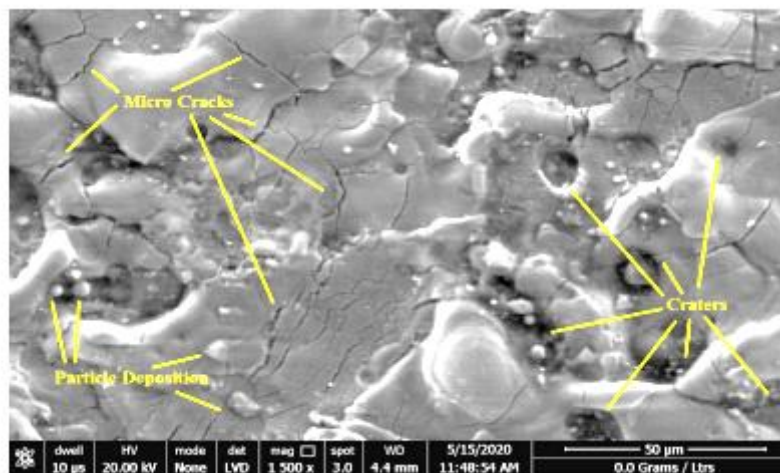


Figure 7(b). The SEM Images after PMEDM with SiC powder.

µm, closely aligning with the predicted values, with less than 5% discrepancies.

Conclusion

This work used PMEDM with SiC powder to investigate how process factors affect the machining properties of a biocompatible Ti-6Al-4V alloy. The analysis and outcomes of the experiment led to the following deductions:

#MRR increases with higher peak current (PC), pulse on time (POT), and powder concentration, while TWR and SR decrease as powder concentration increases.

#The empirical models developed using RSM can accurately predict the machining characteristics, as indicated by the high R² values, demonstrating the models' reliability in forecasting the outcomes.

#Analysis of the surface morphology shows that PMEDM with SiC powder produces surfaces with fewer micro-cracks, smaller craters, and better surface integrity than regular EDM.

#The research provides information for high-quality biomedical implants by identifying the ideal process parameters for machining biocompatible Ti-6Al-4V alloy. To improve PMEDM's use in biomedical engineering, future studies should investigate substitute powder materials such as graphite and aluminum and optimize process parameters for particular biomedical applications.

Acknowledgements

Acknowledge the lab attendants and technicians.

Conflict of interest

No potential conflict of interest was reported by the author(s).

References

- Al-Khazraji, A., Amin, S. A., & Ali, S. M. (2016). The effect of SiC powder mixing electrical discharge machining on white layer thickness, heat flux and fatigue life of AISI D2 die steel. *Engineering Science and Technology, an International Journal*, 19(3), 1400–1415. <https://doi.org/10.1016/j.jestch.2016.01.014>
- Bhattacharya, A., Batish, A., & Kumar, N. (2013). Surface characterization and material migration during surface modification of die steels with silicon, graphite and tungsten powder in EDM process. *Journal of Mechanical Science and Technology*, 27(1), 133–140. <https://doi.org/10.1007/s12206-012-0883-8>
- Das, R., Banerjee, S., & Madhu, U. (2016). Effect of deformation and sensitization on corrosion behavior of 304 LN and 316 LN Austenitic stainless steel. *Int. J. Exp. Res. Rev.*, 4, 1–8.
- Ezugwu, E. O., & Wang, Z. M. (1997). Titanium alloys and their machinability—a review. *Journal of Materials Processing Technology*, 68(3), 262–274. [https://doi.org/10.1016/s0924-0136\(96\)00030-1](https://doi.org/10.1016/s0924-0136(96)00030-1)
- Garg, R. K., Singh, K. K., Sachdeva, A., Sharma, V. S., Ojha, K., & Singh, S. (2010). Review of research work in sinking EDM and WEDM on metal matrix composite materials. *The International Journal of Advanced Manufacturing Technology*, 50(5-8), 611–624. <https://doi.org/10.1007/s00170-010-2534-5>
- Geetha, M., Singh, A. K., Asokamani, R., & Gogia, A. K. (2009). Ti based biomaterials, the ultimate choice for orthopaedic implants – A review. *Progress in Materials Science*, 54(3), 397–425. <https://doi.org/10.1016/j.pmatsci.2008.06.004>
- Ho, K. H., & Newman, S. T. (2003). State of the art electrical discharge machining (EDM). *International Journal of Machine Tools and Manufacture*, 43(13), 1287–1300. [https://doi.org/10.1016/S0890-6955\(03\)00162-7](https://doi.org/10.1016/S0890-6955(03)00162-7)
- Jahan, M. P., Rahman, M., & Wong, Y. S. (2011). A review on the conventional and micro-electrodischarge machining of tungsten carbide. *International Journal of Machine Tools and Manufacture*, 51(12), 837–858. <https://doi.org/10.1016/j.ijmachtools.2011.08.016>
- Jahan, M.P., Rahman, M., Wong, Y.S., & Fuhua, L. (2010). On-machine fabrication of high-aspect-ratio micro-electrodes and application in vibration-assisted micro-electrodischarge drilling of tungsten carbide. *Proceedings of the Institution of Mechanical Engineers, Part B: Journal of Engineering Manufacture*, 224(5), 795–814. <https://doi.org/10.1243/09544054jem1718>
- Jain, S., & Mulewa, A. (2024). Experimental Analysis of Surface Roughness Optimization of EN19 Alloy Steel Milling by the Cuckoo Search Algorithm. *International Journal of Experimental Research and Review*, 38, 102–110. <https://doi.org/10.52756/ijerr.2024.v38.009>
- Jeswani, M. L. (1981). Effect of the addition of graphite powder to kerosene used as the dielectric fluid in electrical discharge machining. *Wear*, 70(2), 133–139. [https://doi.org/10.1016/0043-1648\(81\)90148-4](https://doi.org/10.1016/0043-1648(81)90148-4)
- Kansal, H. K., Singh, S., & Kumar, P. (2005). Parametric optimization of powder mixed electrical discharge machining by response surface methodology. *Journal of Materials Processing Technology*, 169(3), 427–436.

- <https://doi.org/10.1016/j.jmatprotec.2005.03.028>
Kansal, H. K., Singh, S., & Kumar, P. (2006). Performance parameters optimization (multi-characteristics) of powder mixed electric discharge machining (PMEDM) through Taguchi's method and utility concept. *Indian Journal of Engineering and Materials Sciences*, 13(3), 209–216.
- Kansal, H. K., Singh, S., & Kumar, P. (2007a). Effect of Silicon Powder Mixed EDM on Machining Rate of AISI D2 Die Steel. *Journal of Manufacturing Processes*, 9(1), 13–22.
[https://doi.org/10.1016/s1526-6125\(07\)70104-4](https://doi.org/10.1016/s1526-6125(07)70104-4)
- Kansal, H. K., Singh, S., & Kumar, P. (2007b). Technology and research developments in powder mixed electric discharge machining (PMEDM). *Journal of Materials Processing Technology*, 184(1), 32–41.
<https://doi.org/10.1016/j.jmatprotec.2006.10.046>
- Khanra, A. K., Pathak, L. C., & Godkhindi, M. M. (2009). Application of new tool material for electrical discharge machining (EDM). *Bulletin of Materials Science*, 32(4), 401–405.
<https://doi.org/10.1007/s12034-009-0058-0>
- Kumar, P.M., Sivakumar, K., Selvaraja, L. (2024). EDM machining effectiveness for Ti–6Al–4V alloy using Cu–TiB₂ ceramic composite electrode: a parametric evaluation. *Ceramics International*, 50(11B), 2024, 20118-20132.
<https://doi.org/10.1016/j.ceramint.2024.03.135>
- Kumar, V., Hussain, M., Singh, R., & Kumar, S. (2020). Comparison of Process Parameters on Mild Steel and SS304 Through Statistical Analysis of Optimization Technique. *Advanced Science, Engineering and Medicine*, 12(7), 888–893.
<https://doi.org/10.1166/ase.2020.2646>
- Kuriachen, B., & Mathew, J. (2015). Effect of Powder Mixed Dielectric on Material Removal and Surface Modification in Microelectric Discharge Machining of Ti-6Al-4V. *Materials and Manufacturing Processes*, 31(4), 439–446.
<https://doi.org/10.1080/10426914.2015.1004705>
- Lee, H. T., & Tai, T. Y. (2003). Relationship between EDM parameters and surface crack formation. *Journal of Materials Processing Technology*, 142(3), 676–683. [https://doi.org/10.1016/s0924-0136\(03\)00688-5](https://doi.org/10.1016/s0924-0136(03)00688-5)
- Nauryz, N., Omarov, S., Kenessova, A., Pham, T.T., Talamona, D., & Perveen, A. (2023). Powder-Mixed Micro-Electro-Discharge Machining-Induced Surface Modification of Titanium Alloy for Antibacterial Properties. *J. Manuf. Mater. Process*, 7, 214.
<https://doi.org/10.3390/jmmp7060214>
- Niinomi, M. (2008). Mechanical biocompatibilities of titanium alloys for biomedical applications. *Journal of the Mechanical Behavior of Biomedical Materials*, 1(1), 30–42.
<https://doi.org/10.1016/j.jmbbm.2007.07.001>
- Peças, P., & Henriques, E. (2003). Influence of silicon powder-mixed dielectric on conventional electrical discharge machining. *International Journal of Machine Tools and Manufacture*, 43(14), 1465–1471.
[https://doi.org/10.1016/s0890-6955\(03\)00169-x](https://doi.org/10.1016/s0890-6955(03)00169-x)
- Soni, J. S., & G. Chakraverti. (1996). *Experimental investigation on migration of material during EDM of die steel (T215 Cr12)*. 56(1-4), 439–451.
[https://doi.org/10.1016/0924-0136\(95\)01858-1](https://doi.org/10.1016/0924-0136(95)01858-1)
- Sumanth, P., Reddy, M.V., Shaik, I., & Rao Maddu, J.R. (2021). Parameter Optimization of EDM Characteristics on Ti-6Al-4V Using Different Electrodes. *IOP Conf. Ser.: Mater. Sci. Eng.*, 1185, 012022. <https://doi.org/10.1088/1757-899X/1185/1/012022>
- Tzeng, Y.F., & Lee, C.Y. (2001). Effects of Powder Characteristics on Electrodischarge Machining Efficiency. *The International Journal of Advanced Manufacturing Technology*, 17(8), 586–592.
<https://doi.org/10.1007/s001700170142>
- Verma, D., Singh, B., Kumar, A., & Rizvi, S. A. (2024). Assessment of Surface Quality during EDM of AISI 4147 with Copper Tool. *Int. J. Exp. Res. Rev.*, 38, 173-181. <https://doi.org/10.52756/ijerr.2024.v38.016>
- Wu, K. L., Yan, B. H., Huang, F. Y., & Chen, S. C. (2005). Improvement of surface finish on SKD steel using electro-discharge machining with aluminum and surfactant added dielectric. *International Journal of Machine Tools and Manufacture*, 45(10), 1195–1201.
<https://doi.org/10.1016/j.ijmactools.2004.12.005>

How to cite this Article:

Diwaker Tiwari and Ashok Kumar Shrivastava (2024). Process Parameter Effects on Powder Mixed EDM Machining Characteristics Using Biocompatible Ti-6Al-4V Alloy. *International Journal of Experimental Research and Review*, 41(spl.), 01-10.

DOI : <https://doi.org/10.52756/ijerr.2024.v41spl.001>



This work is licensed under a Creative Commons Attribution-NonCommercial-NoDerivatives 4.0 International License.